

Electronic Supporting Information

Mechanistic Insights Into 4-Nitrophenol Degradation and Benzyl alcohol Oxidation Pathways Over MgO/g-C₃N₄ Model Catalyst systems

P.V.R.K. Ramacharyulu, Sk Jahir Abbas, Smruti R. Sahoo, and Shyue-Chu Ke*

Department of Physics, National Dong Hwa University, Hualien 97401, Taiwan.

*E-mail: ke@mail.ndhu.edu.tw; Fax: +886-3-8633690

Table of Contents		
1	TGA Analysis	Figure S1, Page S2
2	Specific Surface Areas of the Catalysts	Figure S2, Page S3
3	FT-IR Spectra of the catalyst samples	Figure S3, Page S3
4	XPS spectra from the as-synthesized MgO/gC ₃ N ₄ catalysts	Figure S4, Page S4
5	Photoluminescence Spectra of the catalysts	Figure S5, Page S5
6	Recyclability Performance of the Catalysts	Figure S5, Page S5
7	Time-resolved EPR Spectra from the Catalysts	Figure S7, Page S7
8	Photocatalytic degradation of MB	Figure S8, Page S9
9	EPR spin trapping with DMPO	Figure S9, Page S10
10	FT-IR of MgO/g-C ₃ N ₄ (1:5) before and after photocatalysis	Figure S10, Page S11
11	Uv-vis absorbance of MgO/g-C ₃ N ₄ (1:5) before and after photocatalysis	Figure S11, Page S11

TGA Analysis

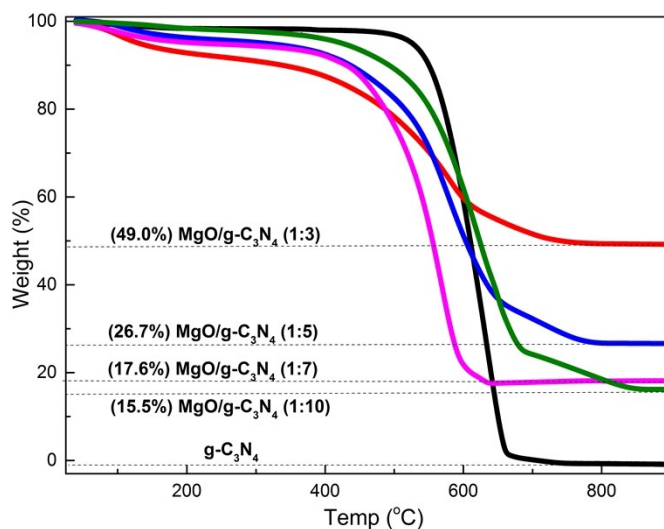


Figure S1: Thermo gravimetric analysis plots of $g\text{-C}_3\text{N}_4$ and $\text{MgO}/g\text{-C}_3\text{N}_4$ catalysts done at a range from 30 – 900°C in ambient environmental conditions. A steep fall in pure $g\text{-C}_3\text{N}_4$ weight loss can be observed in the temperature range from 490°C to 690°C. This indicates its complete decomposition in the temperature range, 490°C to 690°C. On the other hand, $\text{MgO}/g\text{-C}_3\text{N}_4$ catalysts exhibit a gradual weight loss along with reduced decomposition temperatures. MgO concentration in the catalysts was determined from the remaining weight after the curve attained saturation. The respective values for each catalysts are shown in the figure.

Specific Surface Areas of the Catalysts

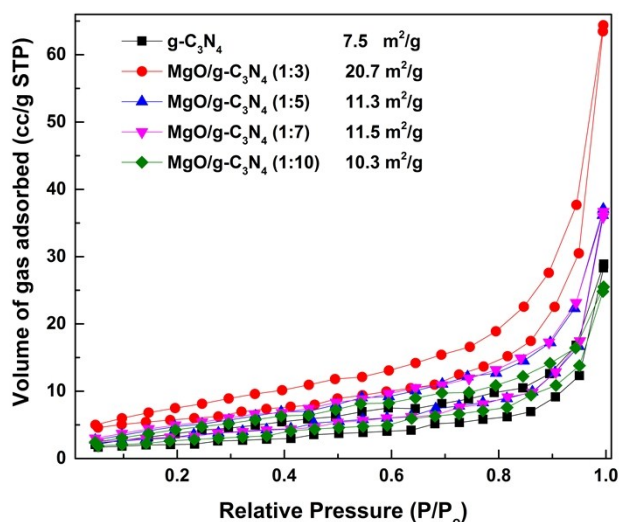


Figure S2. Nitrogen adsorption-desorption measurements of g-C₃N₄ and MgO/g-C₃N₄ composites. The specific surface areas of the respective catalysts are also shown in the figure.

FT-IR Spectra of the catalyst samples

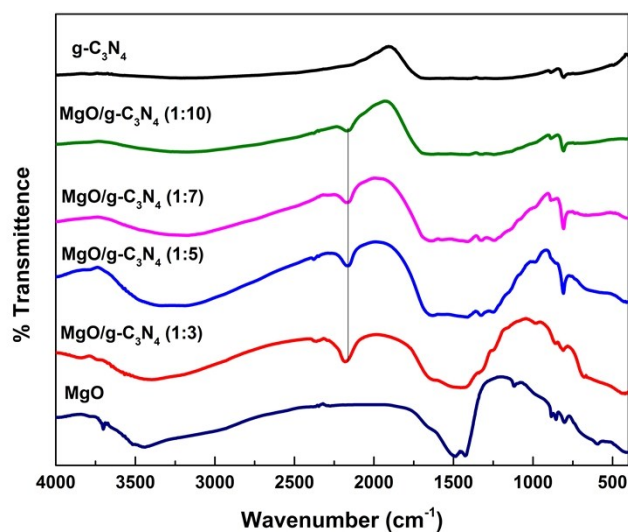


Figure S3. The FT-IR spectra of g-C₃N₄ and MgO/g-C₃N₄ composites exhibit a broad peak at ~3192 cm⁻¹, corresponding to the -N-H stretching vibrations present in primary and secondary

amines.^{1a} The peak at 2160 cm^{-1} is due to the cyano group ($-\text{C}\equiv\text{N}$) or cumulative double bond groups ($-\text{N}=\text{C}=\text{N}-$), present in $\text{g}-\text{C}_3\text{N}_4$. With increase in MgO concentration, this peak both increases in intensity and shifts towards higher wavenumbers. This peak is thus sensitive to any changes in the $\text{g}-\text{C}_3\text{N}_4$ external chemical environment.^{1b} A series of bands in the range of 1600–1200 cm^{-1} are ascribed to the stretching mode of aromatic CN heterocycles. The obvious sharp band at around 808.1–806.1 cm^{-1} relates to the characteristic breathing mode of CN heterocycles of triazine units.^{1c} The shift in the peaks at 2160 and 806 cm^{-1} suggests that, there is some chemical interaction between MgO and $\text{g}-\text{C}_3\text{N}_4$ and is consistent with earlier reports.^{1b}

XPS spectra from the as-synthesized $\text{MgO}/\text{gC}_3\text{N}_4$ catalysts

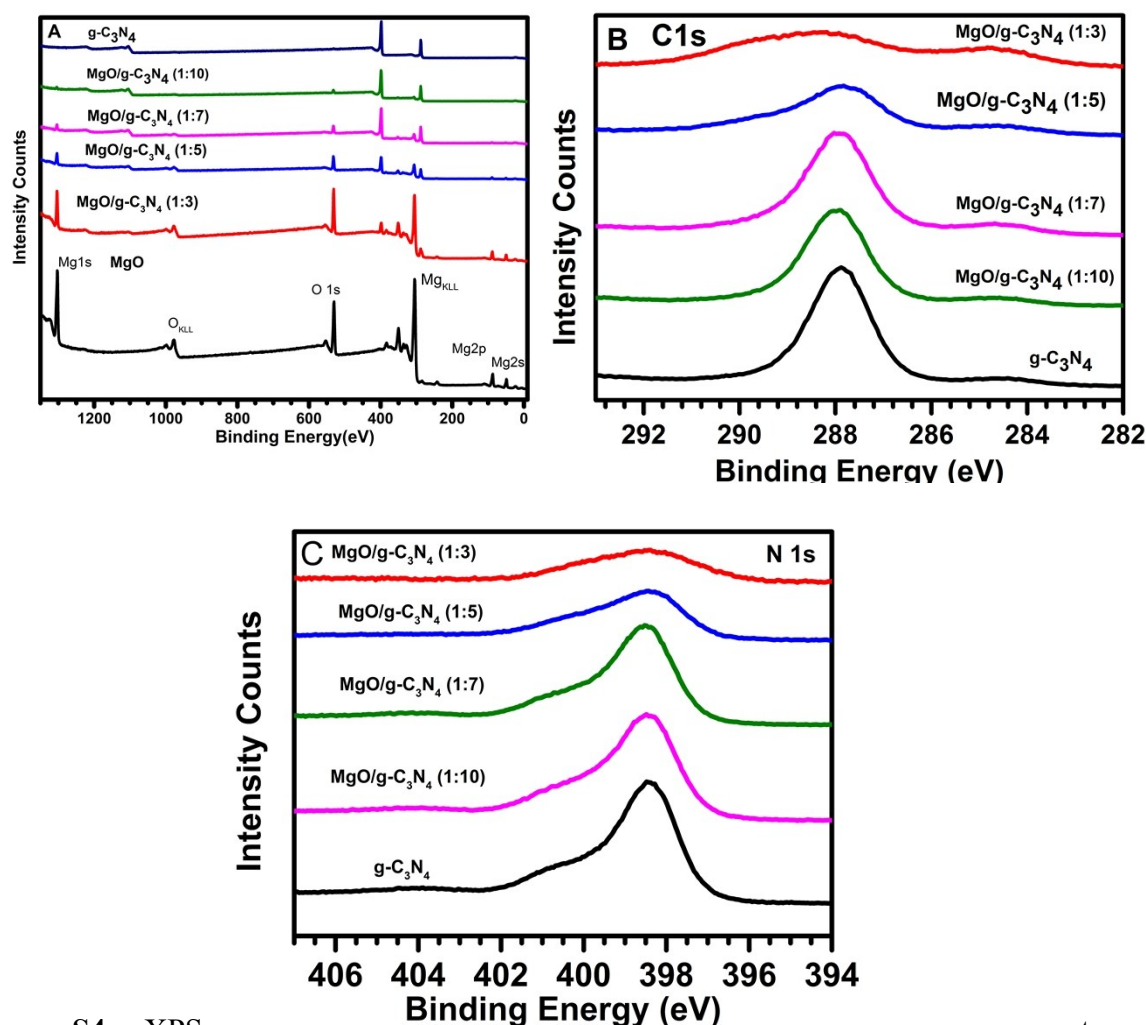


Figure S4. XPS survey spectra of $\text{g}-\text{C}_3\text{N}_4$, MgO , $\text{MgO}/\text{g}-\text{C}_3\text{N}_4$ catalysts at different concentrations (A). $\text{C}1s$ and $\text{N}1s$ core level high resolution XPS spectra of $\text{g}-\text{C}_3\text{N}_4$ as well as $\text{MgO}/\text{g}-\text{C}_3\text{N}_4$ catalysts are also shown in B and C respectively.

Photoluminescence Spectra of the catalysts

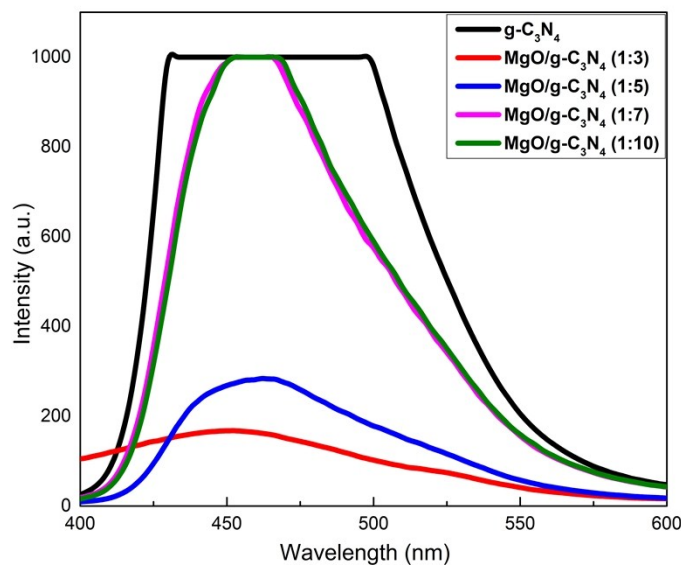


Figure S5. Photoluminescence (PL) spectra of $g\text{-C}_3\text{N}_4$ and $\text{MgO}/g\text{-C}_3\text{N}_4$ composites. $g\text{-C}_3\text{N}_4$ shows highest PL intensity, followed by $\text{MgO}/g\text{-C}_3\text{N}_4$ (1:10), $\text{MgO}/g\text{-C}_3\text{N}_4$ (1:7), $\text{MgO}/g\text{-C}_3\text{N}_4$ (1:5) and $\text{MgO}/g\text{-C}_3\text{N}_4$ (1:3) respectively. This shows the $g\text{-C}_3\text{N}_4$ concentration dependent behavior of PL intensity in the $\text{MgO}/g\text{-C}_3\text{N}_4$ composites. Spectra from $g\text{-C}_3\text{N}_4$, $\text{MgO}/g\text{-C}_3\text{N}_4$ (1:10) and $\text{MgO}/g\text{-C}_3\text{N}_4$ (1:7) composites attained the detector saturation count limits.

The photocatalytic degradation rate of 4-nitrophenol as well as oxidation rate of Benzyl alcohol deviated from this regular trend (Figure 5 & Table 2). The degree of structural imperfection could also induce non-radiative recombination. Therefore, we suggest that PL intensity should not be used as a hallmark feature for implicating the mechanism for enhanced charge carrier separation efficiency.

Recyclability Performance of the Catalysts

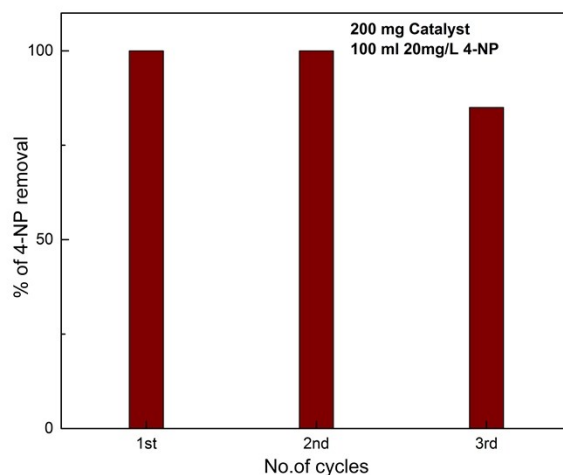


Figure S6. The recyclability performance of MgO/g-C₃N₄ (1:5) catalyst towards 4-nitrophenol degradation. After each set of consecutive experiments, the catalyst was centrifuged, washed with both distilled water and ethanol, and finally dried at 100°C to be subjected to further subsequent runs. Based on the experimental data, the catalyst was stable up to two runs and was found to lose 10 % activity in the third run.

Time-resolved EPR Spectra from the Catalysts

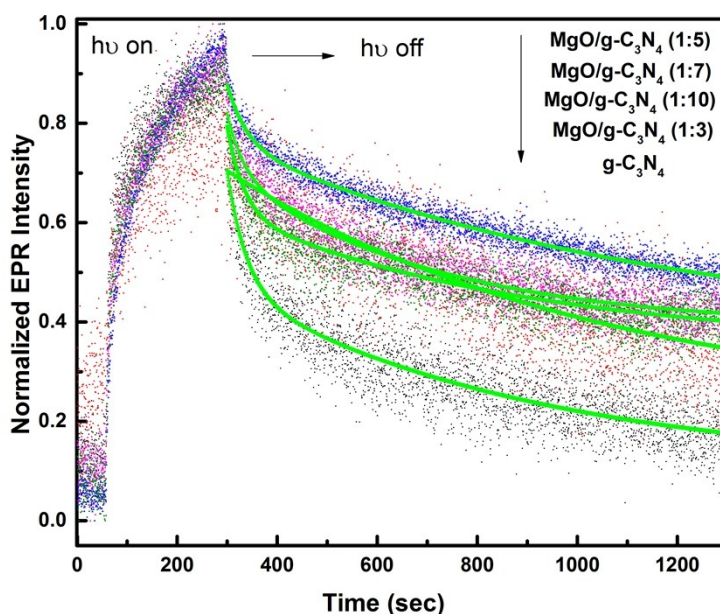


Figure S7. Time resolved EPR tracking spectra of $g\text{-C}_3\text{N}_4$ and $\text{MgO}/g\text{-C}_3\text{N}_4$ composites. This supports the proposed self-trapping mechanism for enhanced charge carrier separation. The data demonstrates the survival of more no. of electrons on $\text{MgO}/g\text{-C}_3\text{N}_4$ than $g\text{-C}_3\text{N}_4$ after light off.

Photocatalytic degradation of MB

The photocatalytic activities of the as prepared $g\text{-C}_3\text{N}_4$ and $\text{MgO}/g\text{-C}_3\text{N}_4$ composites were evaluated by the degradation of MB in aqueous solution under visible LED light irradiation in ambient environmental conditions. First, the influence of both MgO and $g\text{-C}_3\text{N}_4$ on the photocatalytic degradation of MB were studied independently. MgO could not degrade MB quite efficiently as compared to $g\text{-C}_3\text{N}_4$. It might be due to its wide bandgap, inactive under visible light. However, $g\text{-C}_3\text{N}_4$ was observed to degrade MB, yielding a rate constant equivalent to that of P25 under the same experimental conditions ($K_{(g\text{-C}_3\text{N}_4)}$: 0.0016 min^{-1} vs. $K_{(\text{P25})}$: 0.0010 min^{-1}). $\text{MgO}/g\text{-C}_3\text{N}_4$ (1:5 and 1:7) showed rate constants of 0.02073 and 0.0198 min^{-1} respectively, which are almost twelve times higher than both $g\text{-C}_3\text{N}_4$ and P25. This shows that the formation of a heterostructure leads to an enhanced separation of the charge carriers in the composite

materials. The low activity of MgO/g-C₃N₄ (1:3) (K=0.0085 min⁻¹) thus can be related to the low amount of g-C₃N₄ present in the composites. However, high amount of g-C₃N₄ in the MgO/g-C₃N₄ (1:10) (K: 0.0115 min⁻¹) composites also did not assist in enhancing the rate of catalytic activities any further. This suggests that there exists an optimum limit of g-C₃N₄ contents in MgO/g-C₃N₄ catalysts for a highest catalytic activity to take place. To investigate the nature of the photoactive radical species formed in MgO/g-C₃N₄ heterostructures, trapping experiments were performed by using different radical scavengers. EDTA, AgNO₃ and p-BQ were chosen as scavengers for holes, electrons, and superoxide anion radicals respectively. A decrease in MB degradation rate was observed upon adding AgNO₃ and p-BQ during photocatalysis. This indicates the role of electrons acting as active sites towards MB degradation. To investigate the role of holes, EDTA was added during photocatalysis. As is observed from the figure, EDTA addition did not change the degradation rate. Thus the role of holes influencing photocatalytic degradation is ruled out. After each photocatalytic experiment, the catalyst was centrifuged, washed with DI-H₂O, ethanol and dried at 100 °C to be reused for subsequent runs. The used catalysts showed MB degradation performances of 100, 85, 81 and 78% respectively, in sequential runs.

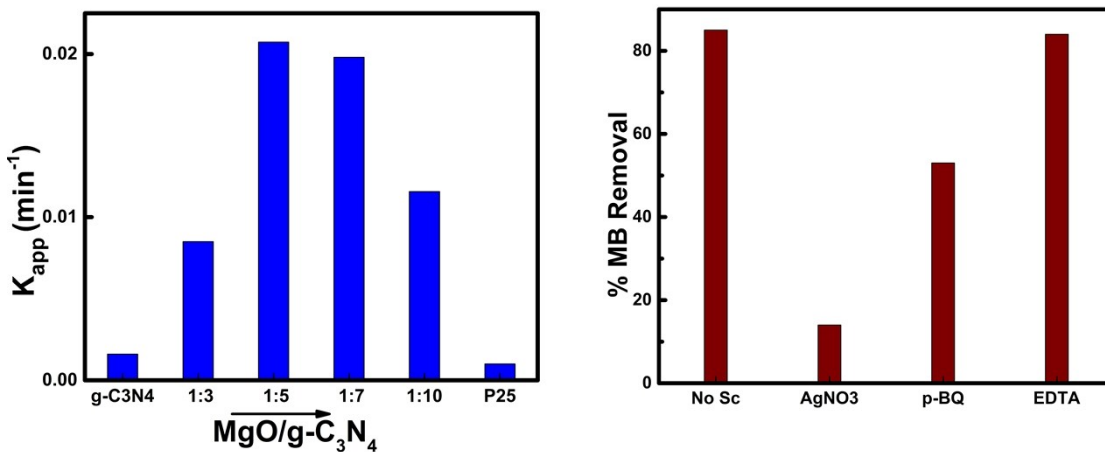


Figure S8. A) Photocatalytic degradation of MB by using g-C₃N₄ and MgO/g-C₃N₄ catalysts; B) Radical scavenging experimental analysis of MB degradation using MgO/g-C₃N₄ catalysts.

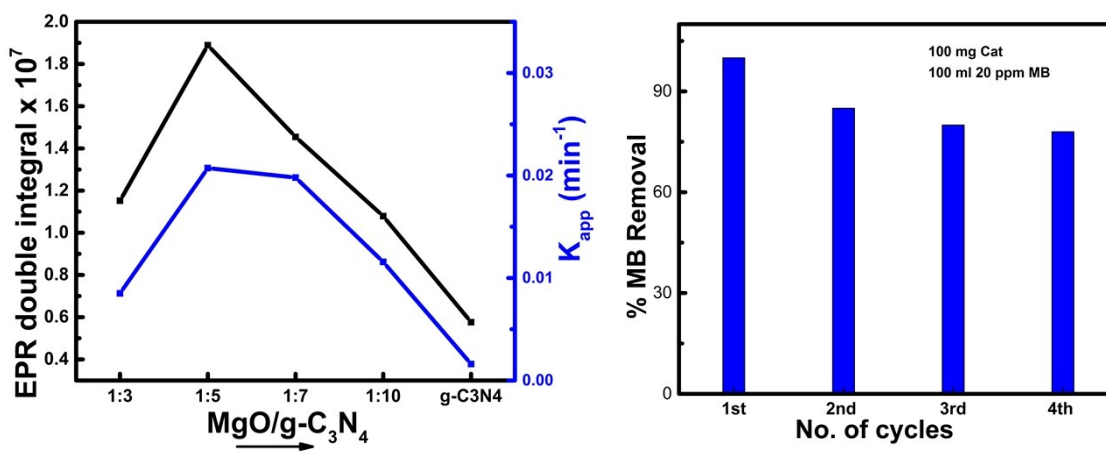


Figure S8. C) Correspondence between the apparent rate constants of MB degradation under visible light, and the double integrated visible light minus dark EPR signal for g-C₃N₄ and MgO/g-C₃N₄ composites. D) Photocatalyst stability and recyclability studies on MgO/g-C₃N₄ catalysts.

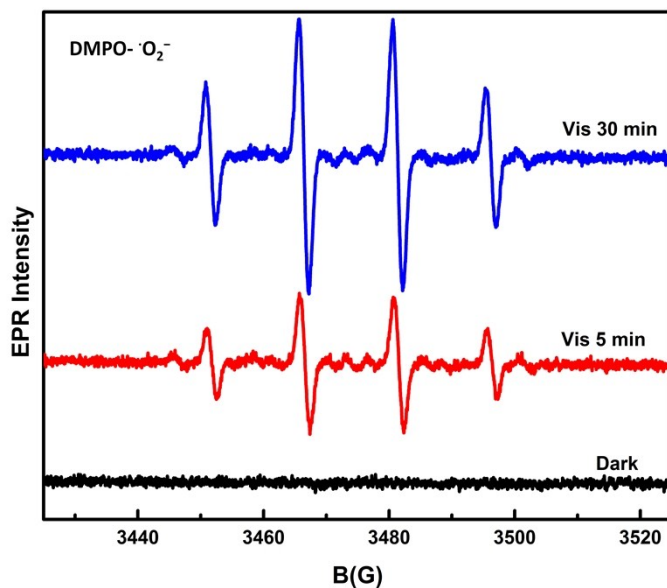


Figure S9. EPR spin-trapping with DMPO demonstrates electron initiated $\cdot\text{O}_2^-$ is the dominant radical photogenerated on MgO/g- C_3N_4 .²

Experimental Conditions: 10 mg of MgO/g- C_3N_4 (1:5) were dispersed in 3 ml DMPO (0.1 M), while being continuously irradiated for 30 min with visible light.

MgO/g- C_3N_4 catalysts were observed to be deactivated after multiple times reuse. This could be due to the strong adsorption of pollutant molecules or residual organic byproducts on the active sites of the catalyst surface in an irreversible manner. Other possible reasons could be due to low light absorption or electron trapping ability.³⁻⁷ The MgO/g- C_3N_4 (1:5) spent catalyst was characterized by UV-Vis and FT-IR spectroscopy.

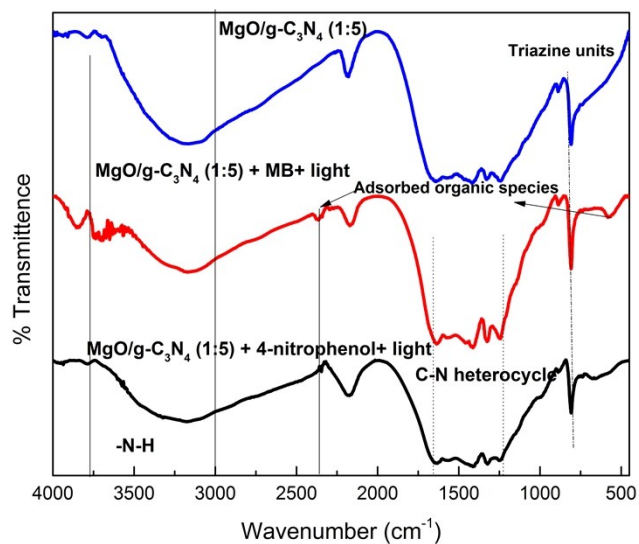


Figure S10. FT-IR of MgO/g-C₃N₄ (1:5) before and after photocatalytic degradation.

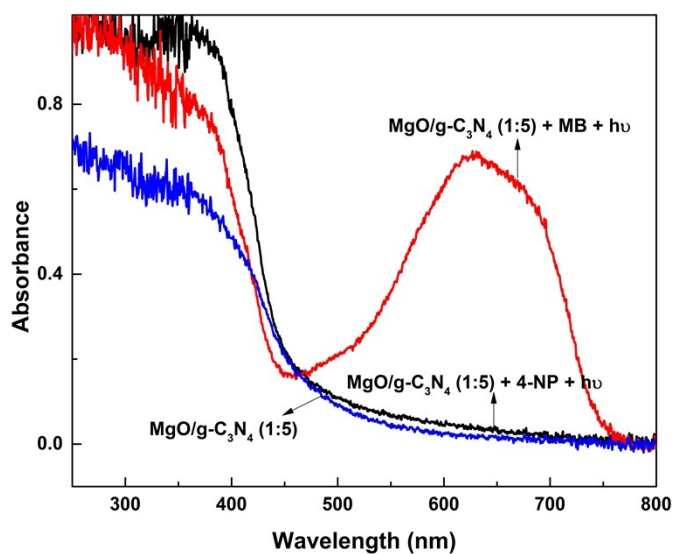


Figure S11. UV-vis of MgO/g-C₃N₄ (1:5) before and after photocatalytic degradation.

References

- 1) a) M.J. Bojdys, J.-O. Müller, M. Antonietti and A.Thomas, Chem. Eur. J., 2008, 14, 8177. b) J. Xu, Y. Chen, D. Ma, J-K. Shang and Y-X. Li, Catal. Comm., 2017, 95, 72. c) S. Samanta, S. Martha and K. Parida, ChemCatChem, 2014, 6, 1453.
- 2) W. Huang, B. C. Ma, H. Lu, R.Li, L. Wang, K. Landfester and K.A.I. Zhang, ACS Catal., 2017, 7, 5438.
- 3) W. Saoud, A. A. Assadi, M. Guiza, A. Bouzaza, W. Aboussaoud, A. Ouederni, I. Soutrel, D. Wolbert and S. Rtimi, Appl. Catal. B: Environ. 2017, 213, 53.
- 4) S. Liu, H. Sun, A. Suvorova and S. Wang, Chem. Eng. J. 2013, 229, 533.
- 5) K.S. Ranjith and R.T. Rajendra kumar, RSC Adv. 2017, 7, 4983.
- 6) Y. Qu, X. Duan, Chem. Soc. Rev. 2013, 42(7), 2568.
- 7) K. Kabra, R. Chaudary, R.L. Sawhney, Ind. Eng. Chem. Res. 2004, 43(24), 7683.